DOI: 10.1002/ejoc.200700293

Why are Phosphole Oxides Unstable? The Phenomenon of Antiaromaticity as a Destabilizing Factor

Zoltán Mucsi*[a] and György Keglevich[a]

Keywords: Phosphole oxide / ab initio DFT calculations / Antiaromaticity / Aromaticity scale

It is shown that the great instability of phosphole oxides can be attributed to their antiaromatic characters. The aromatic–antiaromatic switch in the course of the oxidation of phospholes, which may be fine-tuned by P substituents, increases the reactivity toward dimerisation, leading to the corresponding 7-phosphanorbornene rings. The degree of antiaromaticity of these stable compounds is examined and quantified on a linear aromatic and antiaromatic scale.

1. Introduction

The aromaticity of phospholes has been questionable for a long time,[1,2] and the commonly accepted view is that they have a very weak aromatic character.[3] Earlier studies found that their aromatic stabilization energies (ASEs) are roughly 30–60 kJ mol^{-1}, which is considerably lower[3,4] than in the nitrogen analogue, pyrrole (70–130 kJ mol^{-1}).[3,4] The lack of aromaticity is due to the pyramidal geometry around the P atom; the lone electron pair cannot participate in the delocalization. The high inversion barrier of the phosphorus pyramid prevents inversion or flattening.[2] The weak aromaticity may also be attributed to the hyperconjugation of the exocyclic σ(P–Y) bond.[5] Several studies have found that, in contrast with the stability of phospholes (e.g., **1**), phosphole oxide derivatives (e.g., **2**) exhibit an unusual instability.[6,7] The phosphole oxides obtained on oxidation of the phospholes undergo regio- and stereospecific Diels–Alders-type [4 + 2] dimerization reactions to afford exclusively 7-phosphanorbornene ring systems **3** (Scheme 1).[6,8] A theoretical study showed that the reaction is kinetically controlled and that only one structure **3** with the given configuration can be formed.[9]

Other experimental findings revealed that phospholes **4** are stable for days, but their oxidized derivatives **5** are unstable under the same conditions and are rearranged to **6** (Scheme 2).[7] The instability of **5** was explained by a weak antiaromaticity.[7] These compounds are important, as they can be used as multifunctional materials for organic light-emitting diodes (OLEDs).[10]

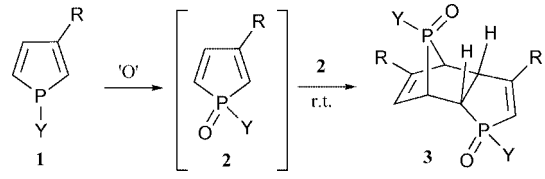

Scheme 1.

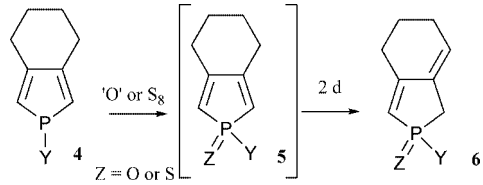

Scheme 2.

It seemed to be interesting to study the theoretical background of the driving force for the classical **1** → **2** → **3** transformation; the phenomenon of antiaromaticity may obviously be an important factor in the reaction sequence. The determination of the antiaromatic character of **2** and **5** by traditional means, however, is not simple. The NICS[11] values show significant deviation from the usual values due to the shielding effect of the P atom,[7] while BIRD indexes[3a] were also found to be unsuitable.[7] It was a challenge for us to elaborate a method for the reliable and quantitative characterization of the antiaromaticity of phosphole chalcogenides.

2. Computation Methods

The B3LYP/6-31G,[12] B3LYP/6-31G(d) and B3LYP/6-311++G(2d,2p) levels of theory were used for this work, with the aid of the Gaussian03 program.[13] The computed enthalpies and Gibbs free energies with respect to the values at 298.14 K are summarized in Table S1.

[a] Department of Organic Chemical Technology, Budapest University of Technology and Economics,
1521 Budapest, Hungary,
Fax: +36-1-4633648
E-mail: zoltanmucsi@gmail.com
Supporting information for this article is available on the WWW under http://www.eurjoc.org or from the author.

3. Results and Discussion

3.1. Quantification of Aromaticity and Antiaromaticity

Levels of antiaromaticity have been quantified in terms of hydrogenation reactions [Figure 1; Equation (1)].[4] The dependent variable *y*, measuring the percentage of aromaticity or antiaromaticity and running between benzene (+100%) and cyclobutadiene (–100%) has been defined as a linear function of the relative enthalpy of hydrogenation [Equation (1) and Equation (2)]. This methodology also requires reference hydrogenation reactions, as shown in Figure 1 for benzene and cyclobutadiene, as well as for **1** and **2**,[4] where $m = 0.6496$ and $b = -1.9273$ at the B3LYP/6-31G(d) level of theory.[4]

$$\Delta\Delta H_{H2} = \Delta H_{H2}[I] - \Delta H_{H2}[II] \quad (1)$$

$$\text{aromaticity/antiaromaticity (\%)} = m\,\Delta\Delta H_{H2} + b \quad (2)$$

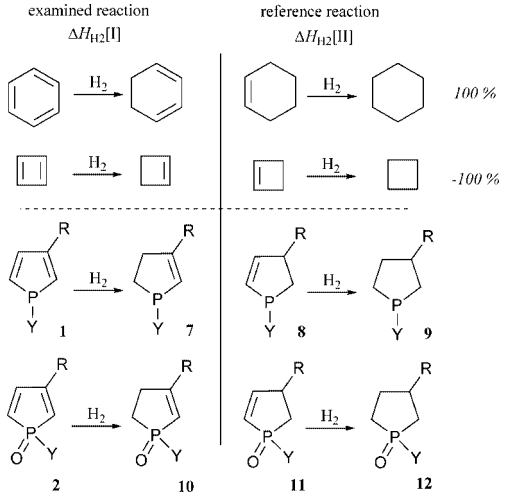

Figure 1. Definition of aromaticity percentages.

The calculated aromaticity and antiaromaticity percentages of **1a**–**e** and **1h**–**l** are summarized in Tables 1 and 2. The values are in good agreement with expectation and the previously reported data.[3,4] As can be seen, phospholes are of weak aromatic character, but in accord with earlier experiences (shown), **1e** (and **1l**) possess the highest aromaticity percentage values (Figure 2).[14] This is due to the flattened P atom, which makes a significant aromatic delocalization possible.[14] The OMe and F substituents (**1f**, **1g**, **1m**, **1n**),

Table 1. Computed $\Delta\Delta H_{H2}$ values (kJ mol^{-1}) and calculated aromaticity/antiaromaticity percentages for compounds **1** at the B3LYP/6-31G(d) level of theory.

Y		R = H $\Delta\Delta H_{H2}$	%		R = Me $\Delta\Delta H_{H2}$	%
H	**a**	31.29	18.40	**h**	16.96	9.09
Me	**b**	21.97	12.34	**i**	21.74	12.20
Ph	**c**	15.70	8.27	**j**	15.25	7.98
2,4,6-Me-C_6H_2	**d**	34.34	20.38	**k**	27.85	16.16
2,4,6-*t*Bu-C_6H_2[a]	**e**	46.65	28.38	**l**	43.33	26.22
OMe	**f**	–4.58	–4.90	**m**	–3.24	–4.03
F	**g**	11.11	–9.15	**n**	–9.62	–8.18

[a] Modelled by a 2,6-di-*tert*-butyl-4-methylphenyl group.

Table 2. Computed $\Delta\Delta H_{H2}$ values (kJ mol^{-1}) and calculated aromaticity/antiaromaticity percentages of compounds **2** at the B3LYP/6-31G(d) level of theory.

Y		R = H $\Delta\Delta H_{H2}$	%		R = Me $\Delta\Delta H_{H2}$	%
H	**a**	–17.12	–13.05	**h**	–33.31	–23.57
Me	**b**	–16.44	–12.60	**i**	–38.83	–27.15
Ph	**c**	–21.84	–16.12	**j**	–37.65	–26.39
2,4,6-Me-C_6H_2	**d**	–23.54	–17.22	**k**	–43.64	–30.27
2,4,6-*t*Bu-C_6H_2[a]	**e**	–12.90	–10.31	**l**	–13.15	–10.47
OMe	**f**	–24.99	–18.16	**m**	–47.05	–32.49
F	**g**	26.54	–19.17	**n**	–43.13	–29.94

[a] Modelled by a 2,6-di-*tert*-butyl-4-methylphenyl group.

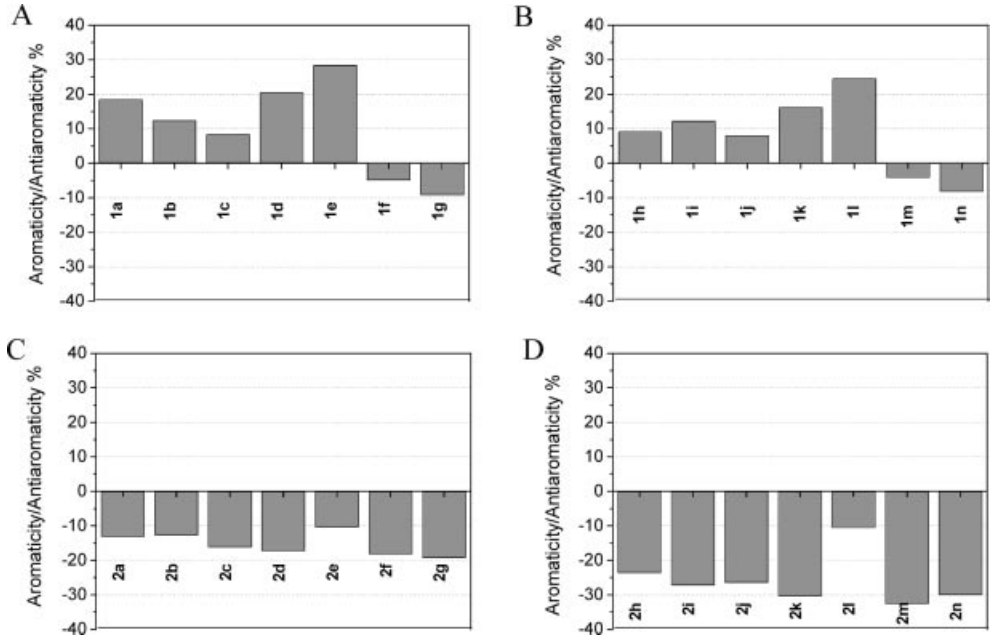

Figure 2. Aromaticity/antiaromaticity diagrams for **1** (A and B) and **2** (C and D) computed at the B3LYP/6-31G(d) level of theory.

however, change the aromaticity to a very weak antiaromaticity, which may explain the failure to prepare these derivatives.

As proposed earlier, the $\sigma^3 \rightarrow \sigma^4$ transformation of the P atom by oxidation switches the weak aromaticity of **1** to a medium antiaromatic character in **2**. It seemed to be interesting to investigate the phosphole chalcogenides (Scheme 3), in which Z = S (**13**) and Se (**14**), and to compare these instances to the Z = O case (**2c**). A significant decrease in the antiaromatic character can be seen in the Z = O, S, and Se periodic order (Figure 3). A more strongly electron-withdrawing atom causes a larger antiaromaticity.

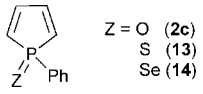

Scheme 3.

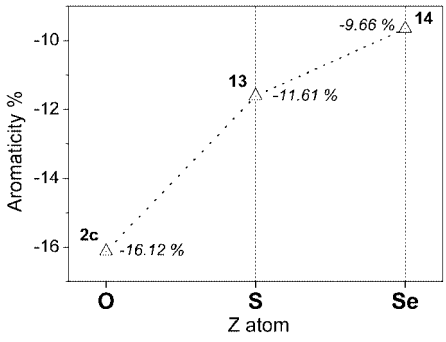

Figure 3. Aromaticity/antiaromaticity percentages of **2c**, **13** and **14**.

The antiaromaticities of **2**, **13** and **14** can be explained by their resonance structures (**I** and **II**), in which **I** and **II** represent a nonaromatic and an antiaromatic ring system, respectively (Figure 4B). Resonance structure **II** contains a P atom with positive charge, which allows continuous 4π-conjugation. This situation shows a close analogy with borole, in which the empty p_z orbital of the B atom plays a role in the antiaromaticity (Figure 4).[15] The "ratio" of resonance structures **I** and **II** results in the final extent of antiaromaticity. A similar situation was revealed earlier in the case of heterophosphetes.[16]

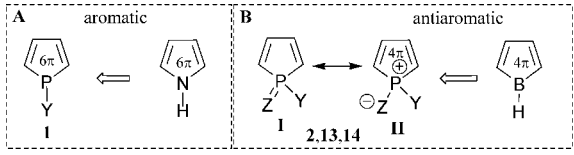

Figure 4. Analogy between A) pyrrole and **1**, and B) borole and **2**, **13** and **14**, with 6π and 4π conjugated electron systems, respectively.

The types of computed molecular orbitals (MOs) for pyrrole, **1a**, **2a** and borole are shown in Figure 5. The MOs and their energy levels of **2a** show a significant correlation with the same MOs of antiaromatic borole; that is, the shapes and symmetries of HOMO – 1, HOMO, LUMO and LUMO + 1 for **2a** are very similar to the corresponding MOs of borole. However, the shapes and symmetries of these MOs in **2a** and **1a** differ markedly from each other, reflecting the different electronic structures and molecular properties. The MOs and the energy levels of **1a** correlate with those of the aromatic pyrrole.

Table 1 shows that the presence of an electron-donating group, such as Y = Me, decreases the antiaromatic character (**2b**, **2i**), in relation to the presence of electron-withdrawing groups, such as Ph and F substituents (**2g**, **2n**). In the case of the Me group, the possible hyperconjugative effect may decrease the antiaromaticity. It worth mentioning that the presence of the strongly electron-donating OMe group causes higher antiaromaticity, which may be ex-

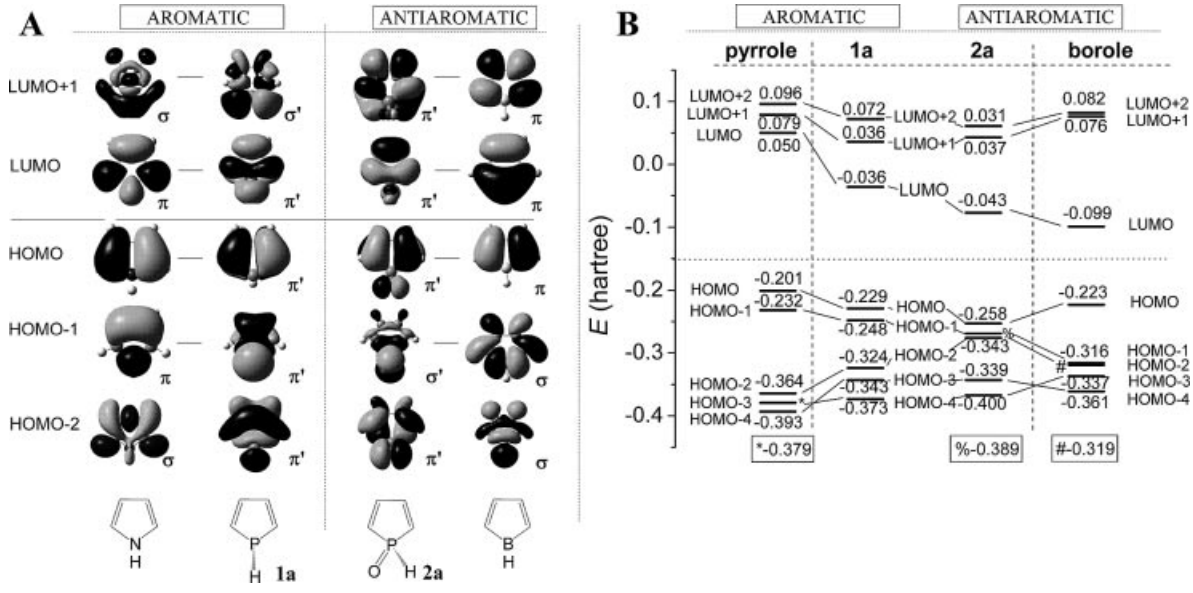

Figure 5. **A**) Schematic representation of selected molecular orbitals of pyrrole, **1a**, **2a** and borole ($\sigma' \rightarrow \sigma$ analogue; $\pi' \rightarrow \pi$ analogue). **B**) Schematic representation of the MO energy levels for pyrrole, **1a**, **2a** and borole computed at the B3LYP/6-31G(d) level of theory.

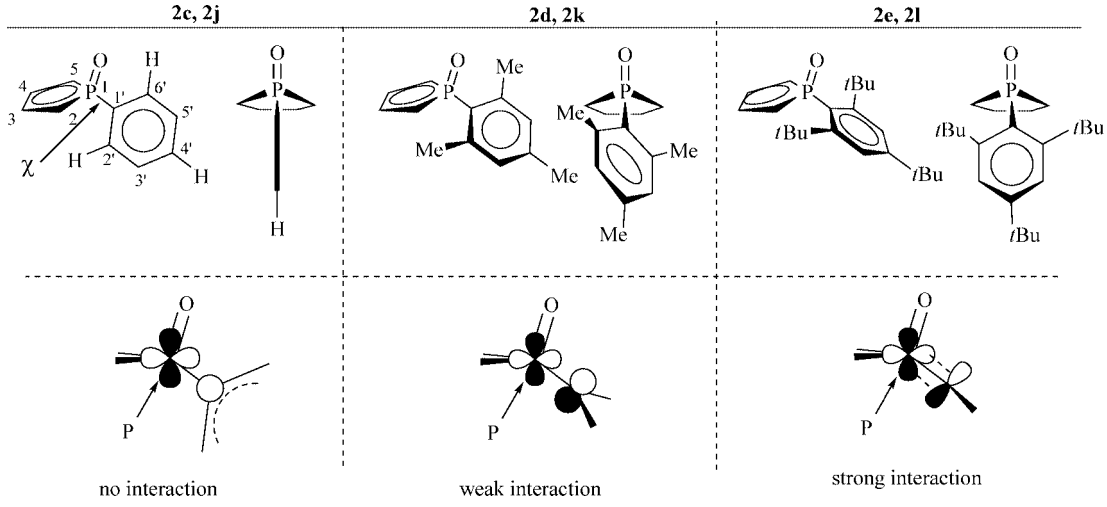

Figure 6. Various arrangements of the substituted phenyl group in **2c**, **2j**, **2d**, **2k**, **2e** and **2l**.

plained by the presence of the electronegative O atom. Only **2e** and **2l** exhibit significantly smaller antiaromatic characters. These lower values can be attributed to the different arrangement of the substituted phenyl group, relative to **2c/2j** and **2d/2k** (Figure 6). When the substituted phenyl group is forced to occupy an orthogonal position to the P=O bond, the p_z atomic orbital on the C^1 atom in the phenyl group is able to overlap with the empty $d_{x^2-y^2}$ or d_{z^2} atomic orbital through combination with p_y of the P atom. This overlap decreases the antiaromaticity of the phosphole ring through charge transfer, because in this special geometry the substituted phenyl group becomes electron-donating towards the electron-deficient P atom, as represented by the resonance structures (**I** and **II**, Figure 6 and Figure 7).

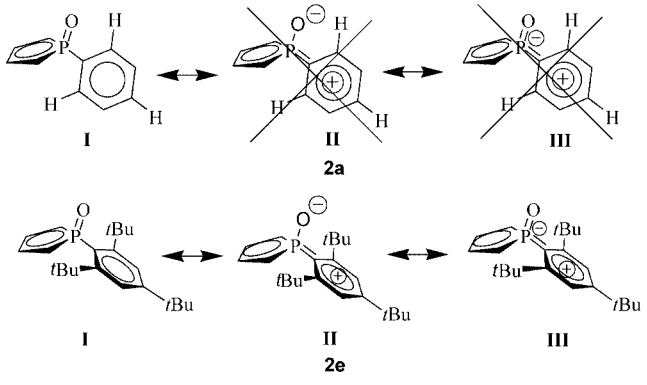

Figure 7. Resonance structures (**I, II** and **III**) of **2c** and **2e**.

In the unsubstituted cases (**2c**, **2j**), the phenyl group is parallel with the P=O bond, so the p_z atomic orbital on C^1 is not able to overlap with the empty $d_{x^2-y^2}$ or d_{z^2} atomic orbitals of the P atom. This type of phenyl group behaves as an electron-withdrawing group, and the second resonance structure (**II**) does not exist (Figure 6 and Figure 7).

To confirm this theory, a rotational experiment was elaborated on molecule **2c**, in which a χ torsion angle is defined by O=P^1–$C^{1'}$–$C^{2'}$ as defined in Figure 6. By rotating the Ph group around the P–C bond from χ = 0°, the conformational minimum of **2c**, to χ = 90° [**2c(90°)**], which is the case in **2e**, one can outline potential energy and antiaromaticity percentage curves correlating with the χ torsion angle (Figure 8). As Figure 9 shows, the rotation curves along the χ

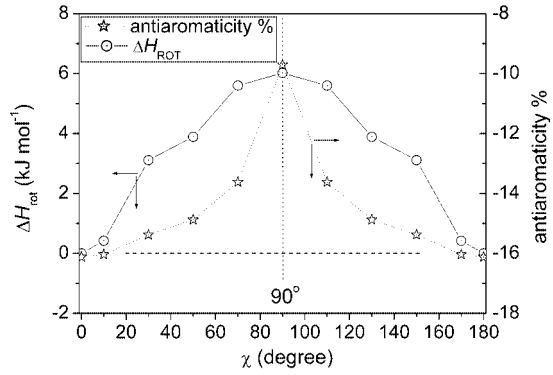

Figure 8. Correlation between conformational energy changes (left, ΔH_{rot}), as well as antiaromaticity percentages (right, %) against χ computed at the B3LYP/6-31G(d) level of theory.

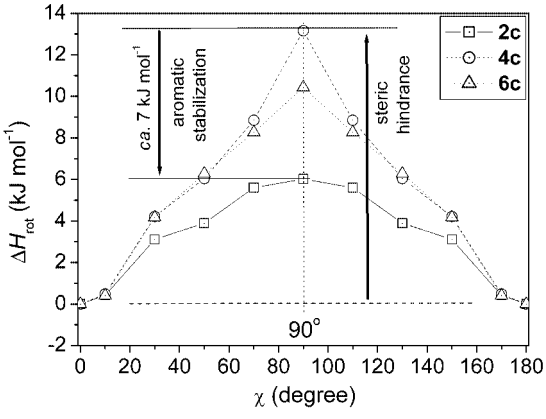

Figure 9. Comparison of the conformational energy changes (ΔH_{rot}) of **2c**, **10c** and **12c** along χ, computed at the B3LYP/6-31G(d) level of theory.

torsion angle for **10c** and **12c** exhibit the higher maximum values, by 4 and 7 kJ mol^{-1}, respectively. The 7 kJ mol^{-1} for **12** is roughly equal with the aromatic stabilization energy (ASE) released during the rotation.

The interaction between the phosphole ring and the Ph ring is depicted in Figure 10, where the two different rotamers [**2c** and **2c(90°)**] exhibit dramatically different MOs (HOMO – 1, HOMO). The overlap between the atomic orbitals of the P and C$^{1'}$ atoms in **2c(90°)** is significant in HOMO – 1, where the corresponding d and p orbitals show significantly higher values than those in **2c**. This overlap between the C and P atomic orbitals may be explained as a charge transfer from the Ph ring to the phosphole oxide ring. It can be represented by the sums of the natural bond orbital (NBO) charges of all atoms involved in the two rings separately (Figure 10). A significant decrease in the group charge (–0.012) for the phosphole oxide can be observed when the χ is turned from 90° to 0°.

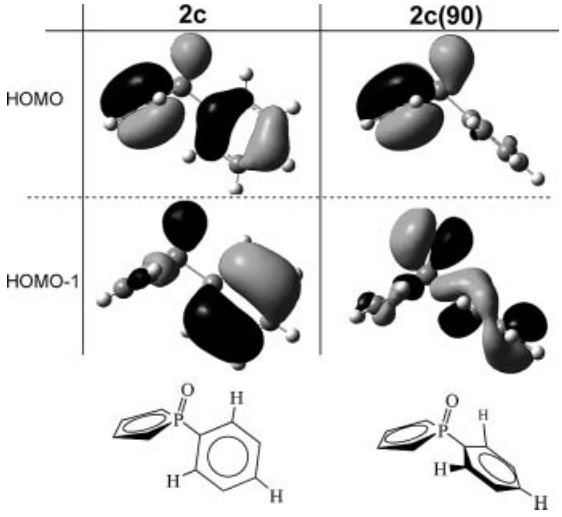

Figure 10. HOMO and HOMO – 1 MOs of **2c** with different χ torsion angles with group NBO charges (in box).

Finally, it is worth mentioning that phosphole oxides with R = Me substituents exhibit significantly larger antiaromaticity percentages than phosphole oxides with R = H substituents (Table 1).

3.2 Energetics of the Reaction Sequence 1 → 2 → 3

In the first step, **1** is oxidized to afford **2**, which is followed immediately by the second step, in which **2** undergoes a Diels–Alder-type [4+2] dimerization leading to **3** (Scheme 1).[6,8] In spite of the formation of the antiaromatic products, the oxidation is highly exothermic [Table S1, ΔG_{ox} = (–270) – (–330) kJ mol^{-1}]. The exothermic formation of an antiaromatic species may be unexpected, but comparison of the range of the $\Delta G_{\mathbf{1}\rightarrow\mathbf{2}}$ values with the $\Delta G_{\mathbf{7}\rightarrow\mathbf{10}}$ and $\Delta G_{\mathbf{9}\rightarrow\mathbf{12}}$ values [Table S1, (–330) – (–370) kJ mol^{-1}] corresponding to the oxidation of **7** and **9** unambiguously reflects the fact that the oxidation of nonaromatic **7** and **9**, yielding the nonantiaromatic **10** and **12**, gives significantly larger ΔG_{ox} values.

The dimerization of the relatively unstable **2** involves one, usually low- or moderate-energy, transition state [Table 3, $\Delta H^{\ddagger}_{dim}$ = 11.55–47.41 kJ mol^{-1}; $\Delta G^{\ddagger}_{dim}$ = 76.15–102.94 kJ mol^{-1}], which allows the reaction to proceed at low temperature (0–10 °C). The large negative entropy change values can be attributed to the bimolecular reaction, but these values may be lower in solution, due to the hindered molecular translation and rotations, relative to the gas-phase situation, lowering the $\Delta G^{\ddagger}_{dim}$ values as well. Both the $\Delta H^{\ddagger}_{dim}$ and the $\Delta G^{\ddagger}_{dim}$ values are in a relatively narrow range. Although the energetics of the reaction explain the process well, one may outline the change in the aromaticity/antiaromaticity along with the reaction profile of the transformation of **1** → **2** → **3** (Figure 11), where the aromatic character of **1** is switched to antiaromatic on oxidation, resulting in **2**. The final product should be **3**, a nonaromatic species because of the four tetrahedral sp^3 C atoms in the framework, discontinuing the conjugated electron system. The antiaromatic characters of phosphole oxides significantly reduce the activation parameters of the dimerization of phosphole oxides, relative to the same dimerization reaction of slightly aromatic phospholes. The difference is ca. 70 kJ mol^{-1} [at the B3LYP/6-31G(d) level of theory]. The disappearance of the antiaromaticity during the reaction can be considered the main driving force, but the steric hindrance has a significant impact as well. In the cases of **2e** and **2l**, the bulky groups significantly increase the activation parameters, which one may expect from their antiaromaticity percentages.[6] Finally, we may conclude that the slow

Table 3. $\Delta H^{\ddagger}_{dim}$, $\Delta G^{\ddagger}_{dim}$ (kJ mol^{-1}) and $\Delta S^{\ddagger}_{dim}$ (J mol^{-1} K^{-1}) values for the dimerisation of **2** at the B3LYP/6-31G(d) level of theory.

Y		R = H							R = Me					
		2 → 3TS			**2 → 3**				**2 → 3TS**			**2 → 3**		
		$\Delta H^{\ddagger}_{dim}$	$\Delta G^{\ddagger}_{dim}$	$\Delta S^{\ddagger}_{dim}$	ΔH_{dim}	ΔG_{dim}	ΔS_{dim}		$\Delta H^{\ddagger}_{dim}$	$\Delta G^{\ddagger}_{dim}$	$\Delta S^{\ddagger}_{dim}$	ΔH_{dim}	ΔG_{dim}	ΔS_{dim}
H	**a**	11.55	76.15	–216.69	–266.65	–202.77	–214.47	**h**	34.34	92.46	–194.94	–258.08	–193.34	–217.33
Me	**b**	16.66	81.57	–217.70	–246.31	–182.85	–213.05	**i**	25.91	88.66	–210.48	–236.96	–172.52	–216.34
Ph	**c**	37.03	97.35	–202.33	–237.78	–165.11	–243.95	**j**	44.03	101.09	–191.38	–227.00	–161.66	–219.35
2,4,6-Me-C_6H_2	**d**	41.58	98.19	–189.85	–250.52	–186.15	–216.13	**k**	42.83	97.83	–190.01	–240.87	–172.52	–216.34
2,4,6-*t*Bu-C_6H_2[a,b]	**e**	41.13	97.01	–182.25	–279.76	–192.45	–291.02	**l**	47.41	100.80	–179.01	–272.88	–186.08	–291.32
OMe	**f**	24.99	85.35	–202.43	–286.35	–221.84	–216.65	**m**	31.33	86.45	–184.89	–277.50	–214.14	–212.76
F	**g**	0.34	99.39	–198.05	–249.77	–185.35	–216.24	**n**	47.17	102.94	–187.05	–239.50	–174.35	–218.71

[a] Modelled by a 2,6-di-*tert*-butyl-4-methylphenyl group. [b] The thermodynamic corrections are calculated at HF/3-21*.

transformation of **2e** and **2l**[6] can be attributed to a slower oxidation process, rather than to the rate of dimerization. The slow oxidation is due to the bulky R substituents, which hinder the oxidation of **1e** and **1l** to **2e** and **2l**.

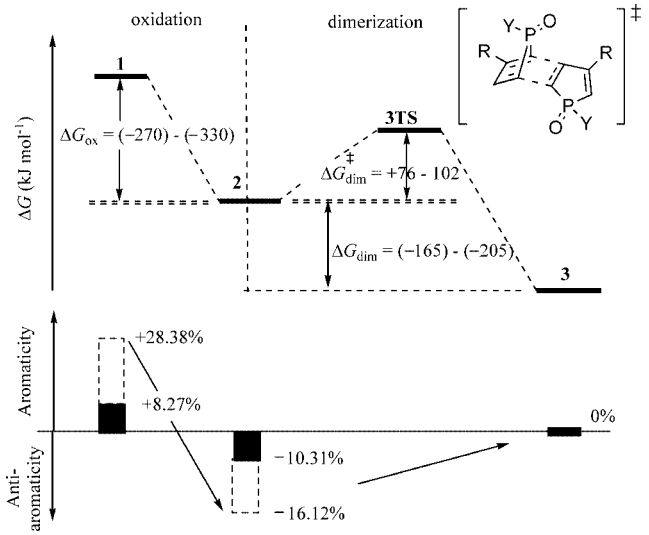

Figure 11. Reaction profile and aromaticity/antiaromaticity profile for the transformation of **1** → **2** → **3**. The dashed boxes indicate the range between the minimum and maximum values computed at the B3LYP/6-31G(d) level of theory.

4. Conclusions

Our results have shown unambiguously that phosphole oxides possess significant antiaromatic character, which can be fine-tuned by the P substituents. Phosphole sulfides and selenides proved to be somewhat less antiaromatic. Depending on the O=P^1–C$^{1'}$–C$^{2'}$ torsion angle, it was shown that a phosphorus-bound phenyl group may behave either as an electron-withdrawing (parallel with P=O), or as an electron-donating group (orthogonal with P=O) toward the P=O group. In the latter case, charge transfer take place from the Ph ring towards the phosphole oxide ring. The antiaromatic characters of phosphole oxides significantly reduce the activation parameters of the dimerization of phosphole oxides, so the driving force of this reaction is the abolition of the antiaromaticity of the starting molecule.

Supporting Information (see also the footnote on the first page of this article): Tables S1–S5 contain the computed energies (*E*), zero point energies (E_{ZPE}), internal energies (*U*), enthalpies (*H*) and Gibbs free energies (*G*) in hartree and entropies (*S*) in cal mol^{-1} K^{-1} at various levels of theories for compounds **1**–**14**. Table S6 shows the *xzy* coordinates of compounds **1** and **2**.

Acknowledgments

The authors acknowledge the support from the Hungarian Scientific Research Fund (OTKA T67679), and thank Imre G. Csizmadia for his assistance in the preparation of this manuscript.

[1] a) L. D. Quin, in *Comprehensive Heterocyclic Chemistry II* (Eds.: A. R. Katritzky, C. W. Rees, E. F. V. Scriven; vol. Ed.: C. W. Bird), vol. 2, Pergamon, Oxford, **1996**, Ch. 15. Phospholes: b) L. D. Quin, in *Phosphorus-Carbon Heterocyclic Chemistry: the Rise of a New Domain* (Ed.: F. Mathey), Pergamon, Amsterdam, **2001**; chapter 4.2.1, chapter 4.2.2. Phospholes: c) F. Mathey, *Chem. Rev.* **1988**, *88*, 429; d) P. v. R. Schleyer, *Chem. Rev.* **2001**, *101*, 1115; e) P. v. R. Schleyer, *Chem. Rev.* **2005**, *105*, 3433.

[2] a) G. Keglevich, in *Targets in Heterocyclic Systems* (Eds.: O. Attanasi, D. Spinelli), Italian Society of Chemistry, **2002**, vol. 6, p. 245; b) N. Mézailles, P. le Floch, *Curr. Org. Chem.* **2006**, *10*, 43; c) F. C. Leavitt, T. A. Manuel, F. Johnson, *J. Am. Chem. Soc.* **1959**, *81*, 3163; d) L. D. Quin, J. G. Bryson, *J. Am. Chem. Soc.* **1967**, *89*, 5984; e) H. Kaye, *J. Am. Chem. Soc.* **1970**, *92*, 5779; f) W. Egan, R. Tang, G. Zon, K. Mislow, *J. Am. Chem. Soc.* **1971**, *93*, 6205; g) I. G. Csizmadia, A. H. Cowley, M. W. Taylor, S. Wolfe, *J. Chem. Soc. Chem. Commun.* **1974**, 432–433.

[3] a) C. W. Bird, *Tetrahedron* **1985**, *41*, 1409; b) M. H. Palmer, R. H. Findlay, *J. Chem. Soc. Perkin Trans. 2* **1975**, 974; c) M. H. Palmer, R. H. Findlay, J. A. Gaskell, *J. Chem. Soc. Perkin Trans. 2* **1974**, 420.

[4] Z. Mucsi, B. Viskolcz, I. G. Csizmadia, *J. Phys. Chem. A* **2007**, *111*, 1123–1132.

[5] a) L. Nyulászi, *Chem. Rev.* **2001**, *101*, 1229; b) W. Schafer, A. Schweig, F. Mathey, *J. Am. Chem. Soc.* **1976**, *98*, 407; c) D. Delaere, A. Dransfeld, M. T. Nguyen, L. G. Vanquickenborne, *J. Org. Chem.* **2000**, *65*, 2631; d) E. Mattmann, F. Mathey, A. Sevin, G. Frison, *J. Org. Chem.* **2002**, *67*, 1208; e) L. Nyulászi, *J. Phys. Chem.* **1995**, *99*, 586; f) L. Nyulászi, *Tetrahedron* **2000**, *56*, 79; g) F. G. N. Cloke, P. B. Hitchcock, P. Hunnable, J. F. Nixon, L. Nyulászi, E. Niecke, V. Thelen, *Angew. Chem. Int. Ed.* **1998**, *37*, 1083.

[6] a) L. D. Quin, *Rev. Heteroat. Chem.* **1990**, *3*, 39; b) G. L. D. Quin, *The Heterocyclic Chemistry of Phosphorus*, Wiley Interscience, New York, **1981**, pp. 79, ch. 2; c) Keglevich, L. Tőke, Zs. Böcskei, V. Harmat, *Heteroat. Chem.* **1997**, *8*, 527; d) L. D. Quin, *Heteroat. Chem.* **1991**, *2*, 359.

[7] L. Nyulászi, O. Hollóczki, C. Lescop, M. Hissler, R. Réau, *Org. Biomol. Chem.* **2006**, *4*, 996.

[8] a) F. Mathey, *Top. Phosphorus Chem.* **1980**, *10*, 43; b) D. A. Usher, F. H. Westheimer, *J. Am. Chem. Soc.* **1964**, *86*, 4732; c) R. Kluger, F. Kerst, D. G. Lee, E. A. Dennis, F. H. Westheimer, *J. Am. Chem. Soc.* **1967**, *89*, 3919; d) G. Keglevich, L. Tőke, K. Újszászi, K. Ludányi, *Heteroat. Chem.* **1996**, *7*, 337; e) G. Keglevich, K. Ludányi, L. D. Quin, *Heteroat. Chem.* **1997**, *8*, 135; f) L. D. Quin, K. C. Caster, J. C. Kisalus, K. Mesch, *J. Am. Chem. Soc.* **1984**, *106*, 7021; g) Y.-Y. H. Chiu, W. N. Lipscomb, *J. Am. Chem. Soc.* **1969**, *91*, 4150; h) L. D. Quin, J. Szewczyk, A. T. McPhail, *J. Org. Chem.* **1986**, *51*, 3341.

[9] Gy. M. Keserű, G. Keglevich, *J. Organomet. Chem.* **1999**, *586*, 166.

[10] C. Fave, T.-Y. Cho, M. Hissler, J. Rault-Berthelot, R. Réau, *J. Am. Chem. Soc.* **2003**, *125*, 9254.

[11] P. v. R. Schleyer, C. Maerker, A. Dransfeld, H. Jiao, N. J. R. von E. Hommes, *J. Am. Chem. Soc.* **1996**, *118*, 6317–6318.

[12] a) P. J. Stephens, F. J. Devlin, C. F. Chabalowski, M. J. Frisch, *J. Phys. Chem.* **1994**, *98*, 11623–11627; b) A. D. Becke, *J. Chem. Phys.* **1993**, *98*, 5648–5651.

[13] M. J. Frisch, G. W. Trucks, H. B. Schlegel, G. E. Scuseria, M. A. Robb, J. R. Cheeseman, V. G. Zakrzewski, J. A. Montgomery, R. E. Stratmann, Jr., J. C. Burant, S. Dapprich, J. M. Millam, A. D. Daniels, K. N. Kudin, M. C. Strain, O. Farkas, J. Tomasi, V. Barone, M. Cossi, R. Cammi, B. Mennucci, C. Pomelli, C. Adamo, S. Clifford, J. Ochterski, G. A. Petersson, P. Y. Ayala, Q. Cui, K. Morokuma, D. K. Malick, A. D. Rabuck, K. Raghavachari, J. B. Foresman, J. Cioslowski, J. V. Ortiz, A. G. Aboul, B. B. Stefanov, G. Liu, A. Liashenko, P.

Piskorz, I. Komaromi, R. Gomperts, R. L. Martin, D. J. Fox, T. Keith, M. A. Al-Laham, C. Y. Peng, A. Nanayakkara, M. Challacombe, P. M. W. Gill, B. Johnson, W. Chen, M. W. Wong, J. L. Andres, C. Gonzalez, M. Head-Gordon, E. S. Replogle, J. A. Pople, *Gaussian 03* 6.0, Gaussian, Inc., Pittsburgh PA, **2003**.

[14] G. Keglevich, Zs. Böcskei, Gy. M. Keserű, K. Újszászi, L. D. Quin, *J. Am. Chem. Soc.* **1997**, *119*, 5095.

[15] M. K. Cyrański, P. v. R. Schleyer, T. M. Krygowski, H. Jiao, G. Hohlneicher, *Tetrahedron* **2003**, *59*, 1657.

[16] Z. Mucsi, T. Körtvélyesi, B. Viskolcz, I. G. Csizmadia, T. Novák, G. Keglevich, *Eur. J. Org. Chem.* **2007**, 1759.

Received: April 2, 2007
Published Online: July 25, 2007

